JOURNAL OF THERMOPHYSICS AND HEAT TRANSFER
Vol. 15, No. 1, January–March 2001

Homogenization of Temperature-Dependent Thermal Conductivity in Composite Materials

Peter W. Chung* and Kumar K. Tamma†
University of Minnesota, Minneapolis, Minnesota 55455
and
Raju R. Namburu‡
U.S. Army Research Laboratory, Aberdeen Proving Grounds, Maryland 21005

Of the various homogenization approaches, the asymptotic expansion homogenization (AEH) approach for homogenizing nonlinear composite material properties continues to grow in prominence due to its ability to handle complex microstructural shapes while relating continuum fields of different scales. The objective is to study the AEH approach for nonlinear thermal heat conduction with temperature-dependent conductivity. First, two approaches are proposed to investigate the sensitivity of the homogenized conductivity to higher-order terms of the asymptotic series. Under conditions of symmetry such as in unidirectional composites, the two approaches give the same homogenized properties. Then validations are shown for unidirectional composites for changing volume fraction and temperature. The validations are performed using measurements and analytical formulas available in the literature. The findings show good agreement between the present numerical predictions and independent results. Finally, a simple nonlinear steady-state heat conduction problem is demonstrated to illustrate the multi-scale procedure. The numerically predicted results are verified using a Runge–Kutta solution.

Introduction

THE study of composite materials and their associated boundary value problems (BVPs) requires the solution of coupled hierarchical differential equations. Moving between these equations entails homogenization (moving from micro to macro) or localization (macro to micro).

The types of problems encountered in the analysis of composite materials are usually over ranges of temperatures or structural behavior that make the problems nonlinear. In contrast to the various traditional approaches to homogenizing multiphase properties, recent developments in the asymptotic expansion homogenization (AEH) approach are useful but formidable for studying nonlinear problems possessing heterogeneous microstructures. Bensoussan et al.[1] and Sanchez-Palencia[2] provide many of the rigorous fundamental mathematical and analytical developments of the AEH approach in a seamless manner. Thermal problems were first treated analytically by early mathematical investigations[1,2] with emphasis on applicability to mostly linear situations. In the area of stress analysis of heterogeneous structures, investigations by Bendsöe and Kikuchi[3] and Lene[4] have successfully extended the approach to more practical engineering applications.

The AEH approach provides localization capability together with homogenization, and, therefore, inherently quantifies the continuum fields over multiple length scales. Homogenization and localization comprise the two main components in a multiscale approach. The former provides a smeared set of properties to be used in the macrofield equations, and the latter provides an estimate of microlevel information based on the macrofield solution. This is what makes AEH more attractive than traditional and so-termed homogenization-only approaches. The benefits of the multiscale capabilities of AEH for nonlinear local effects have been demonstrated only recently in stress analysis.[5–8] Although limited developments are available in homogenization of linear conductivity,[9,10] no efforts to date have treated the nonlinear temperature dependence of conductivity or shown how such approaches substantiate the results.

In the present paper, we describe two multiscale approaches employing AEH for studying the effective properties of materials with nonlinear thermal conductivity. They differ in the manner in which they compute local temperatures. The developments are based on the general localization given by the form

$$T^{\text{micro}} = T^c + T^p \tag{1}$$

where T^c is the centroid temperature of the macro finite element and T^p is the perturbation temperature or microtemperature variation. Then we demonstrate the validity of the proposed developments by comparing with experimental data and analytical methods available in the literature. Finally, an example problem is shown to illustrate the multiscale approach in a nonlinear heat-conduction problem involving temperature-dependent conductivity.

Overview

The AEH approach is based on the assumption that the inhomogeneous material with its intricate microstructure is replaced by a homogeneous body X, whose effective properties are obtained from a scaled microlevel repeating unit cell Y (Fig. 1), with given constituents. The repetition of the cell implies periodicity and requires symmetry conditions to be imposed at the boundaries of Y. The details of the formulation are given elsewhere,[1] and only cursory formulations important and pertinent to the present developments are described.

The coordinate systems for Y and X are defined, respectively, as y_i and x_i (for $i = 1, 2, 3$, assuming three dimensions) and the microstructure scaling is characterized by $y_i = x_i/\varepsilon$, where ε is the scale parameter. At least two finite element (FE) models are required: the first for the macrolevel problem X^e and the second for the representative microlevel unit cell Y^e. This indirectly implies that two equations must be solved via the FE method. One governs the macrolevel and the other governs the microlevel. We assume for simplicity that there is a unique unit cell. A unique unit cell, however, is not a crucial assumption in the approach.

Presented as Paper 99-0878 at the AIAA 37th Aerospace Sciences Meeting, Reno, NV, 11–14 January 1999; received 5 April 1999; revision received 10 April 2000; accepted for publication 10 April 2000.

*Graduate Research Assistant, Department of Mechanical Engineering, 111 Church Street, SE.
†Professor, Department of Mechanical Engineering, 111 Church Street, SE; ktamma@tc.umn.edu. Member AIAA.
‡Research Engineer, Computational and Information Sciences Directorate.

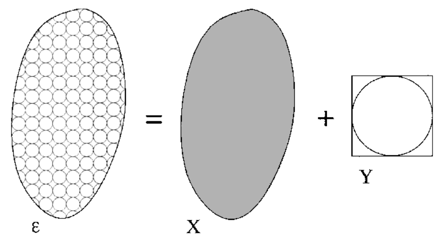

Fig. 1 Body in ε space is the realistic representation of the heterogeneous structure; macro- and microscales are, respectively, modeled with a homogenized body in X and a representative unit cell in Y.

The method is based on the conventional macrolevel problem given as[1]

$$K^\varepsilon(T)T = f_i \quad \text{in} \quad X \tag{2}$$

where T is subject to conditions on ∂X and where the macrolevel temperature field is $T(x_i)$ and, in accordance with existing notation,[1] $K^\varepsilon(T)$ is a differential operator defined by

$$K^\varepsilon(T) = -\frac{\partial}{\partial x_i}\left[k_{ij}\left(\frac{\boldsymbol{x}}{\varepsilon}, T\right)\frac{\partial}{\partial x_j}\right] \tag{3}$$

where we have used boldface first-order tensor notation to avoid confusion with indices. The material properties are defined in the conductivity tensor $k_{ij}(T)$ and are also temperature dependent in the most general case. The true temperature field T^ε or the temperature in the ε body shown in Fig. 1 is expanded asymptotically as

$$T^\varepsilon = T^{(0)}(\boldsymbol{x},\boldsymbol{y}) + \varepsilon T^{(1)}(\boldsymbol{x},\boldsymbol{y}) + \varepsilon^2 T^{(2)}(\boldsymbol{x},\boldsymbol{y}) + \cdots \tag{4}$$

where the superscript on each temperature denotes the order of the asymptotic series, T^ε is the exact temperature being approximated, and ε is a scaling parameter proportional to the ratio of the scales.

The salient feature of the AEH derivation is the development of three hierarchical equations emanating from factoring common orders of ε to yield

$$K_1 T^{(0)} = 0 \tag{5}$$

$$K_1 T^{(1)} + K_2 T^{(0)} = 0 \tag{6}$$

$$K_1 T^{(2)} + K_2 T^{(1)} + K_3 T^{(0)} = f_i \tag{7}$$

where K_1, K_2, and K_3 are temperature-dependent differential operators given by

$$K_1(T^\varepsilon) = -\frac{\partial}{\partial y_i}\left[k_{ij}(\boldsymbol{y}, T^\varepsilon)\frac{\partial}{\partial y_j}\right]$$

$$K_2(T^\varepsilon) = -\frac{\partial}{\partial y_i}\left[k_{ij}(\boldsymbol{y}, T^\varepsilon)\frac{\partial}{\partial x_j}\right] - \frac{\partial}{\partial x_i}\left[k_{ij}(\boldsymbol{y}, T^\varepsilon)\frac{\partial}{\partial y_j}\right]$$

$$K_3(T^\varepsilon) = -\frac{\partial}{\partial x_i}\left[k_{ij}(\boldsymbol{y}, T^\varepsilon)\frac{\partial}{\partial x_j}\right] \tag{8}$$

where $\boldsymbol{y}$ denotes the variation of a quantity over the unit cell Y.

Equation (6) gives the so-called auxiliary equation

$$K_1(T^\varepsilon)\chi^j = -\frac{\partial}{\partial y_i}k_{ij}(\boldsymbol{y}, T^\varepsilon) \tag{9}$$

where χ^j is the corrector function that accounts for the presence of heterogeneities in Y. If one replaces T^ε in Eq. (9) with T^{micro} in Eq. (1), it is clear that the auxiliary function χ depends on the temperature field in Y. One can make a further simplification and assume that the auxiliary function depends only on the macrofield temperature $T^{(0)}$, presently assumed to be the centroid temperature T^c of the macro-FE. Thus, the auxiliary function is the solution of the differential equation

$$K_1\left(T^{(0)}\right)\chi^j = -\frac{\partial}{\partial y_i}k_{ij}\left(\boldsymbol{y}, T^{(0)}\right) \tag{10}$$

Then the perturbation temperature $T^{(1)}$ is given by

$$T^{(1)}(\boldsymbol{x},\boldsymbol{y}) = -\chi^j(\boldsymbol{y})\frac{\partial T^{(0)}}{\partial x_j}(\boldsymbol{x}) + \tilde{T}^{(1)}(\boldsymbol{x}) \tag{11}$$

where $\boldsymbol{x}$ is the variation of a quantity over the macrobody X and $\tilde{T}^{(1)}$ is a constant of integration chosen to be zero. Detailed treatments of this constant can be found in Ref. 1. It is then immediately clear that Eq. (10) is the linearized form of the microequation because χ is independent of $T^{(1)}$.

The nonlinear form is inspired by assuming χ depends on both $T^{(0)}$ and $T^{(1)}$. This is represented by

$$K_1\left(T^{(0)}, T^{(1)}\right)\chi^j = -\frac{\partial}{\partial y_i}k_{ij}\left(\boldsymbol{y}, T^{(0)}, T^{(1)}\right) \tag{12}$$

Note that T^p from Eq. (1) is equivalent to $\varepsilon T^{(1)}$ in Eqs. (4) and (12).

The linear and nonlinear equations given in Eqs. (10) and (12), respectively, comprise the two approaches presently suggested for treating temperature-dependent steady-state thermal conductivity. It is implied that the macrolevel equations are nonlinear regardless of whether the microlevel equations (10) or (12) are linear or nonlinear. In a later section, illustrative cases will demonstrate differences between the approaches.

Note that a true micro/macrotemperature solution is given by using up to second-order terms in Eq. (4) with the result from Eq. (11). This gives the approximation to second order

$$T^\varepsilon(\boldsymbol{x},\boldsymbol{y}) \approx T^c + T^p = T^{(0)}(\boldsymbol{x}) - \varepsilon\left[\chi^j(\boldsymbol{y})\frac{\partial T^{(0)}}{\partial x_j}(\boldsymbol{x})\right] \tag{13}$$

where T^p is neglected in the linear approach only. Employing Eq. (11) in Eq. (7) and noting that

$$\int_Y K_1 T^{(2)}\,\mathrm{d}\boldsymbol{y} = 0 \tag{14}$$

finally leads to the solution for χ, which can be employed to compute the effective conductivity of the unit cell

$$\bar{k}(T^\varepsilon)_{ij} = \frac{1}{|Y|}\int_Y\left[k_{ij}(\boldsymbol{y}, T^\varepsilon) - k_{ik}(\boldsymbol{y}, T^\varepsilon)\frac{\partial\chi^j}{\partial y_k}\right]\mathrm{d}Y \tag{15}$$

with appropriate substitutions for T^ε according to the linear or nonlinear approaches described earlier. As indicated in Eqs. (10) and (12), material nonlinear behavior may be present at the micromechanical level. This nonlinearity affects the macrolevel behavior via the effective conductivity computed in Eq. (15), which depends on the micromechanical corrector function χ^j.

In the general case where the macrolevel problem is nonisothermal, temperature gradients in an element are nonzero, and the results will differ from the isothermal results. Equation (4) indicates that the extent of this difference depends on the parameter ε, which is a measure of the relative sizes of the macro- and microscales. The smaller the magnitude of ε, the smaller the influence of the macrolevel temperature gradients on the microscale homogenized properties. Under certain conditions, the difference between the approaches is nominal. Conditions when the linearized and nonlinear homogenization equations yield identical or nearly identical results are 1) the microstructural geometry contains symmetries, 2) the material is homogeneous, 3) $\partial T^{(0)}/\partial x = 0$, and 4) $\varepsilon \lll 1$.

In summary, the steps in the proposed linear and nonlinear computational procedures are enumerated as follows.

Linear

The linear approach assumes that the temperatures are constant in Y. The procedure for determining the homogenized conductivity in a finite element sense is as follows:

1) Compute the macrotemperature distribution.

2) Determine the element average (at centroid or integration points) temperatures for each macrolevel element.

3) Determine the individual phase conductivities at the average temperature at each microlevel element.

4) Solve the auxiliary equation (10) for χ^j using the conductivities from step 3.

5) Use the solution for χ^j in Eq. (15) to determine the effective conductivity of the macroelement.

Nonlinear

The nonlinear approach makes no restrictions on the temperature distribution in Y. This results in a nonlinear dependence of the homogenized conductivity on the local temperature fields. The procedure to determine the effective conductivity is as follows:

1) Compute the macrotemperature distribution.

2) Determine the element average (or centroid or integration points) temperatures for each macrolevel element.

3) Solve for χ^j in Eq. (12) using the conductivity values for the present iteration.

4) Determine the microscale temperatures using the first two terms in Eq. (4).

5) Update the conductivities of the constituents using the microscale temperatures.

6) Loop back to step 1 until χ^j converges.

7) The effective conductivity is then computed from the converged corrector functions χ^j.

Results and Discussion

Comparisons Between the Linear and Nonlinear Approaches

To further demonstrate the extent of departure of nonlinear thermal conductivities from conventional micromechanical understanding, an example problem is posed. The fiber geometries typically encountered in knitted, woven, or general textiles used in advanced composites can have significant asymmetries that may give different results for the two approaches. Using the linear and nonlinear homogenization approaches, comparisons are presented of the three-dimensional conductivity tensors for a unit cell containing an asymmetrically shaped fiber. It will be shown that for most practical situations, the linear approach can be employed without significant loss of accuracy.

The FE mesh of the micromechanical geometry is shown in Fig. 2a, and a cutaway to show the fiber geometry is shown in Fig. 2b. The geometry shown is representative of microstructures encountered in textile and fabric composites. The nominal fiber value fraction is 32.13%. Whereas unidirectional composites are transversely isotropic, the present example is orthotropic. The HTS DX210/$BF_3$400 composite material properties are used.[11]

A macrolevel BVP must be solved for the nonlinear approach due to its dependence on the macrotemperature gradient. A one-dimensional problem is idealized using three-dimensional hexahedral elements for illustration. Temperature conditions are applied to both ends ($T = \{175.5, 250\}$); for illustration let $\varepsilon = 0.001$, and the steady-state problem is solved via FE analysis. The transverse surfaces are adiabatic.

Figure 3 shows the homogenized conductivities in the x and y directions as a function of the ratio of the fiber to matrix conductivities. It also shows the trends of the homogenized behavior for variations in the constituent properties.

Table 1 Computed effective conductivities as a function of temperature

	Linear method			Nonlinear method		
T,K	k_{xx}	k_{yy}	k_{zz}	k_{xx}	k_{yy}	k_{zz}
246.8	0.43941	0.42892	3.1605	0.43968	0.42931	3.1611
240.3	0.43148	0.42130	3.1079	0.43182	0.42179	3.1085
233.7	0.42337	0.41351	3.0386	0.42369	0.41397	3.0391
226.9	0.41543	0.40588	2.9518	0.41574	0.40633	2.9522
219.8	0.40768	0.39845	2.8444	0.40800	0.39890	2.8449
212.5	0.39919	0.39031	2.7333	0.39952	0.39080	2.7337
204.9	0.39012	0.38162	2.6094	0.39041	0.38204	2.6098
196.9	0.38032	0.37223	2.4822	0.38059	0.37262	2.4826
188.5	0.36991	0.36229	2.3576	0.37016	0.36264	2.3579
179.6	0.35978	0.35262	2.2135	0.36002	0.35296	2.2139

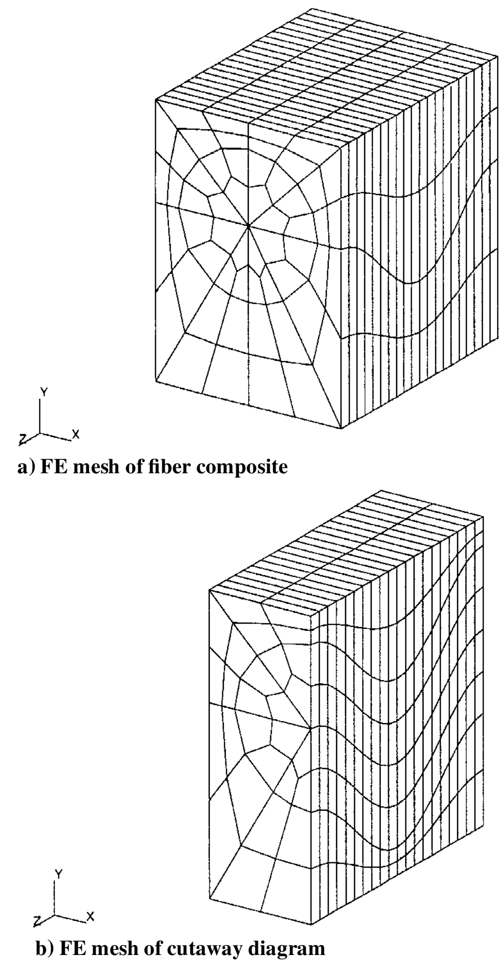

Fig. 2 Unit cell of an asymmetric fiber composite.

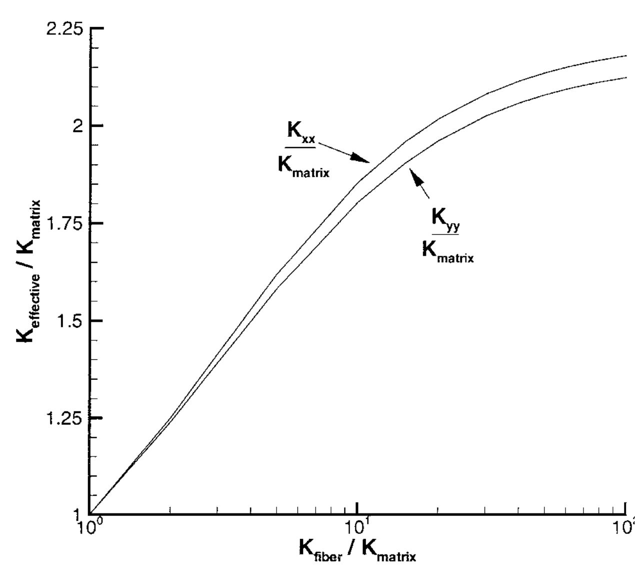

Fig. 3 Homogenized transverse conductivities for asymmetric fiber.

Table 1 shows that the linear and nonlinear homogenization approaches give different numerical results. This is the result foreseen earlier, that the geometric asymmetry or eccentricity causes conductivities obtained from the approaches to be different. However, it is also evident that these differences, occurring at the third or fourth decimal place, approach a level of numerical triviality. Thus, reasonable accuracy can be achieved through the simpler linear approach.

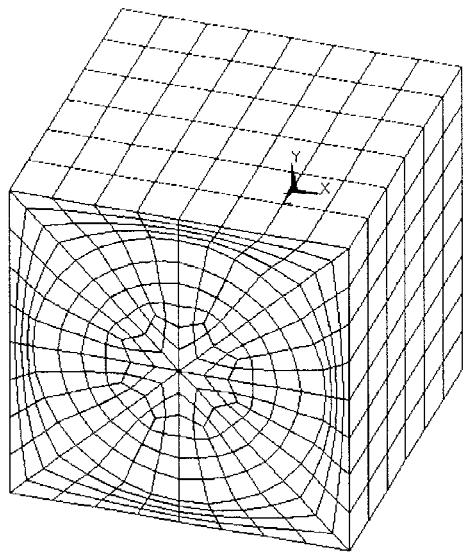

Fig. 4 FE mesh for a unidirectional composite ($V_f = 0.719$) using 3839 nodes and 3280 hexahedral elements.

Validation with Available Experimental Measurements

Validation with experimental measurements[11,12] and analytical formulas[13,14] available in the literature was performed for the effective conductivities using the linear and nonlinear micromechanics approaches. The experimental data and formulas are for cylindrical fibrous composites. The inherent symmetries of such problems cause the two approaches to give the same results because of the inherent thermal loads imparted on the microstructure. These loads cancel in an average sense when the microstructure contains symmetries, and no distinction between the two approaches will be made henceforth.

Note that the difficulty in measuring raw fiber data leads most investigators to backcalculate the fiber conductivity from effective conductivity measurements using rule of mixture-type analytical expressions. In the experimental literature used for comparisons, some form of backcalculation is evident. It is prudent to recognize that the AEH results based on the backcalculated constituent properties will yield homogenized properties different from the measurements. These comparisons with experiments, therefore, show agreement with simple unidirectional composites and, based on these validations for simple geometries, demonstrate the potential to predict the homogenized conductivities for more sophisticated composites.

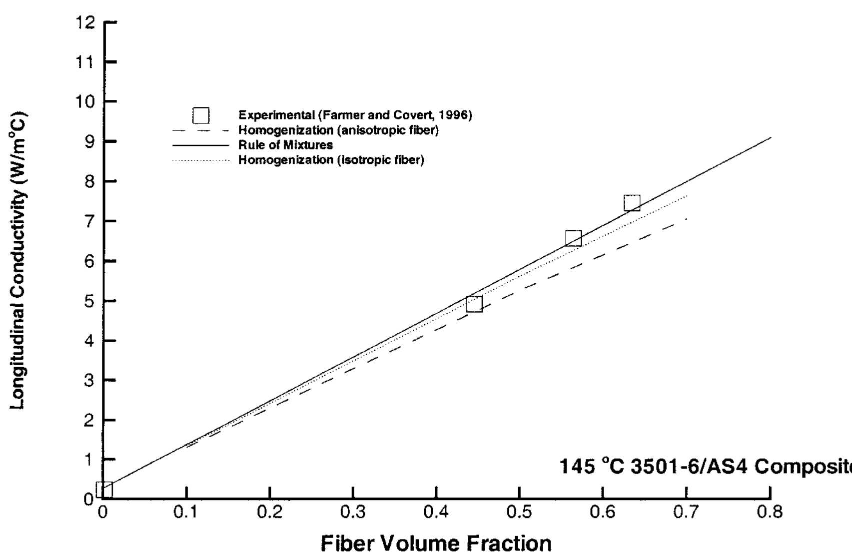

a) Longitudinal conductivity of AS4/3501-6

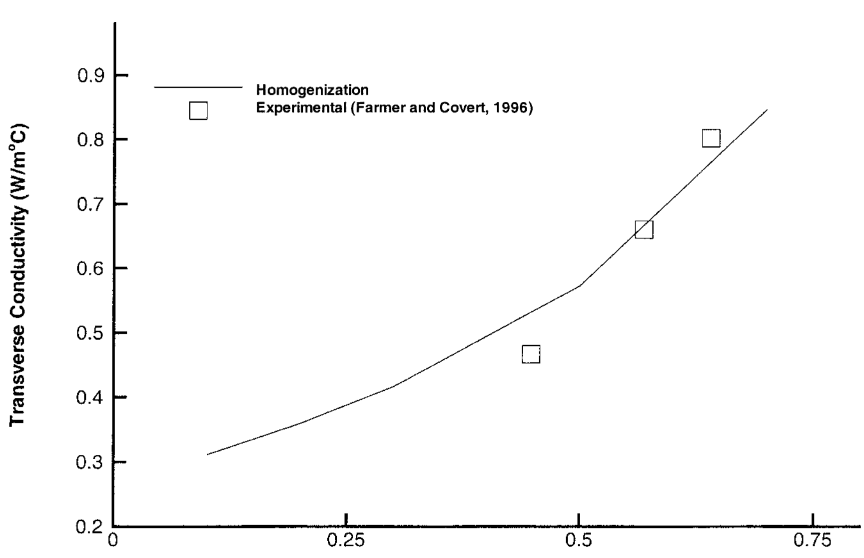

b) Transverse conductivity of AS4/3501-6

Fig. 5 Comparisons of the homogenized conductivities at 145°C for AS4/3501-6 composites using asymptotic expansion homogenization and experimental measurements.

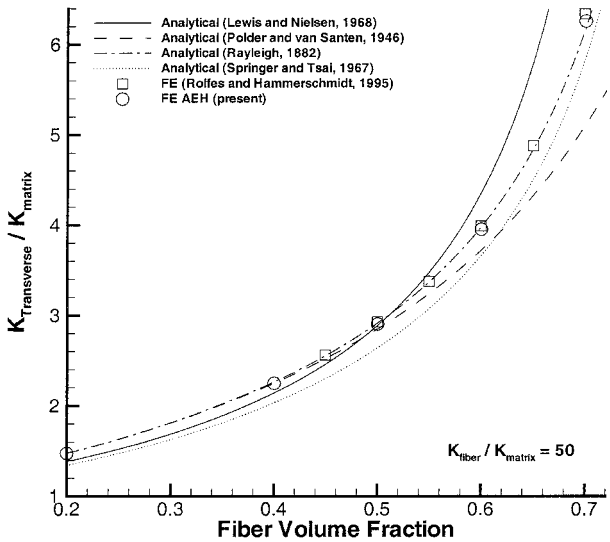

a) **Transverse conductivity of a fibrous composite with $K_{\text{fiber}}/K_{\text{matrix}} = 50$**

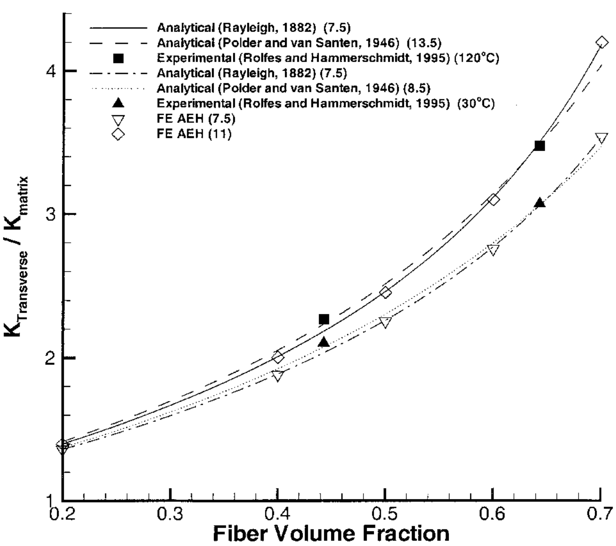

b) **Values (given in parentheses) of either $K_{\text{fiber}}/K_{\text{matrix}}$ ratio or the temperature used in experiment[14]**

Fig. 6 AEH approximation formulas and experimental data.[14]

A volume fraction study was first performed using meshes of the type shown in Fig. 4 for varying fiber diameter. The assumed form of the fiber array is square for illustration purposes. Pilling et al.[11] show that hexagonal packing exerts little influence on the effective conductivity for volume fractions smaller than 70%. The largest volume fraction used in this investigation was 71.9%. Realistically, however, arrangements are closer to a hexagonal array due to the lower potential energy associated with its packing. For the present comparisons, the differences appear to be very small at the volume fractions considered. Comparisons with experiment are shown in Figs. 5a and 5b compared with the numerically predicted conductivities using AEH for AS4/3501-6 composite.[12] AEH was also compared with analytical formulas[13,15–17] which are presented in a review paper with some experimental data.[14] These results are plotted in Figs. 6a and 6b. Very good agreements are shown.

Temperature-dependent conductivity calculations are shown in Figs. 7–9 with comparisons with experiments in independent investigations.[11,12] Material properties are for AS4/3501-6 and HTS/DX210/$BF_3$400 composites. Better agreement was obtained for longitudinal (axial) conductivity than the transverse conductivity. This is a direct consequence of using backcalculated transverse fiber data in the present homogenization approach. Discrepancies such as in Fig. 9 may be attributed to this cause, as well as the inaccuracy of using the square fiber arrangement assumption for high-volume fraction composites.

Verification with Macrolevel Analytical Solution

To demonstrate the AEH procedure, a simple problem is proposed that is verified with a one-dimensional solution. In contrast to the earlier homogenization considerations that are concerned primarily with the calculations over the microstructure, this example attempts to consider the fundamental micro- and macroscales in the same context. The one-dimensional problem is a unidirectional composite with the fibers oriented along its length as shown in Fig. 10 with a fiber volume fraction of 71.9%. The two approaches described earlier give the same results for this example because of the symmetry of the microstructure.

The in-axis temperatures for the two solutions are shown in Fig. 11a. The one-dimensional nonlinear equation was solved via a fourth-order Runge–Kutta scheme using a curve fit for the computed homogenized conductivities. The one-dimensional equation is given as

$$\frac{\partial}{\partial x}\left[k(T)\frac{\partial T}{\partial x}\right] = 0 \tag{16}$$

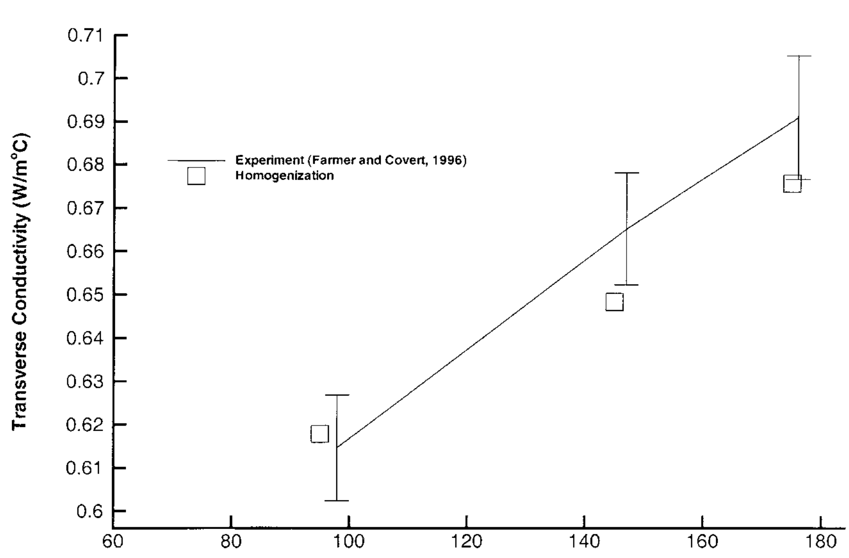

Fig. 7 Temperature-dependent transverse thermal conductivity of AS4/3501-6 with $V_f = 0.57$; comparison between asymptotic expansion homogenization and measurements.[12]

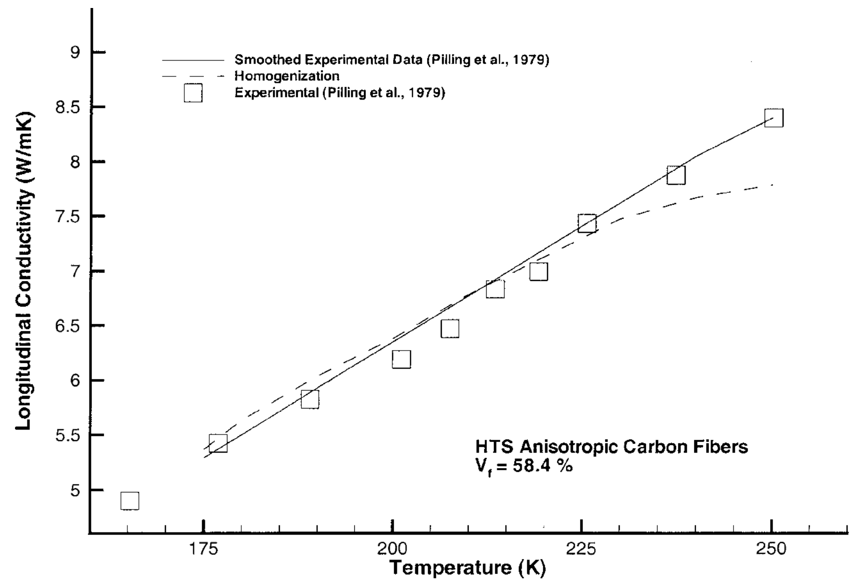

HTS DX210/BF$_3$400 with $V_f = 0.584$

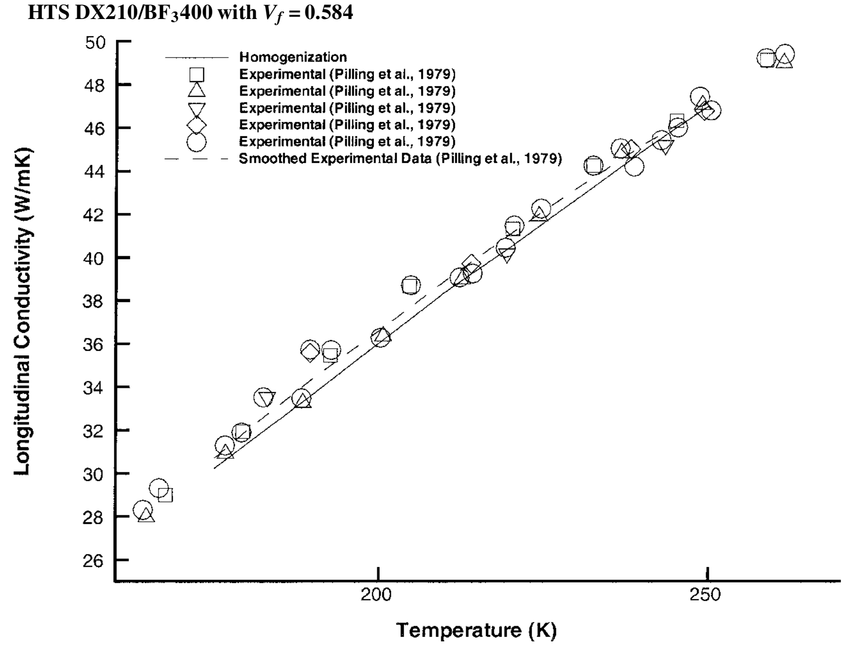

HMS DX210/BF$_3$400 with $V_f = 0.607$

Fig. 8 Temperature-dependent longitudinal thermal conductivity; comparison between AEH and measurements.[11]

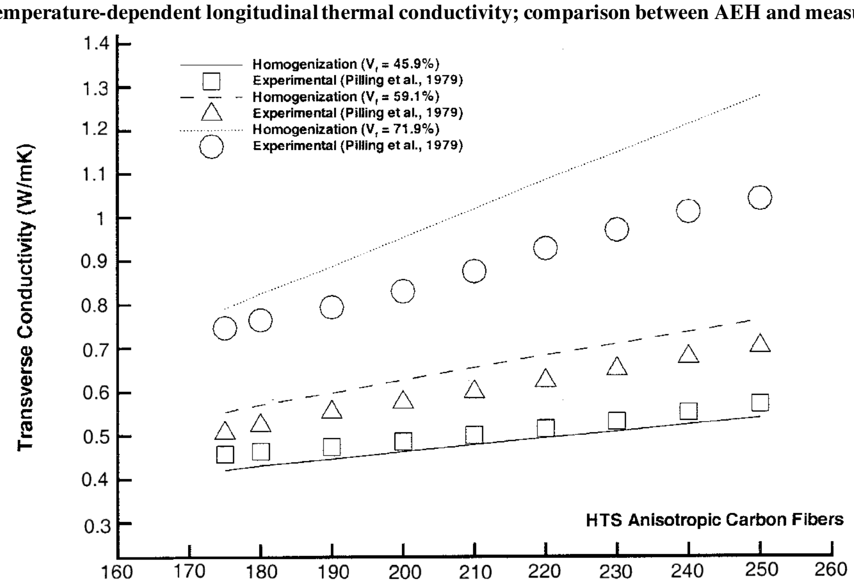

Fig. 9 Temperature-dependent transverse thermal conductivity of HTS DX210/BF$_3$400 at various volume fractions; comparisions between AEH and measurements.[11]

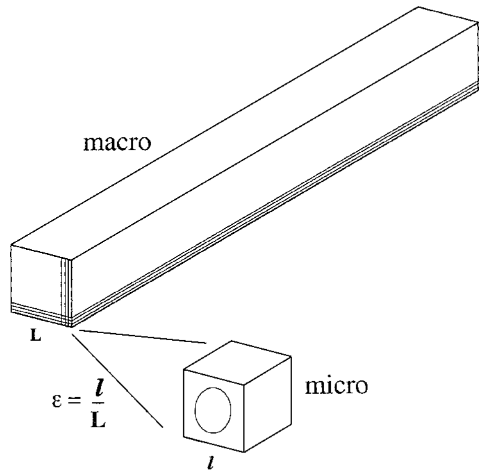

Fig. 10 Macro- and microgeometries for a continuous-fiber unidirectional composite with fibers aligned along the length.

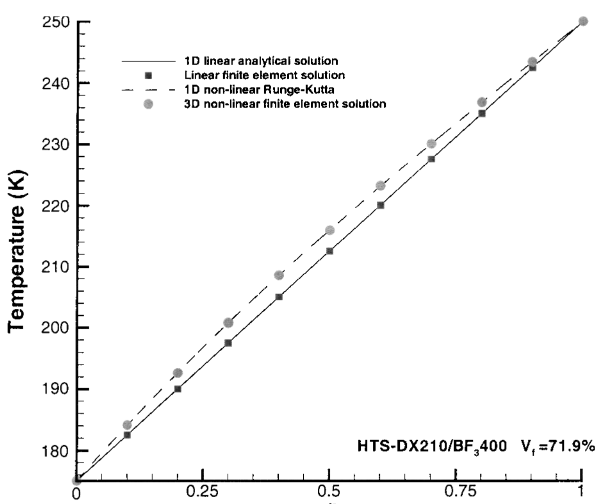

a) Temperature solutions for linear and nonlinear cases

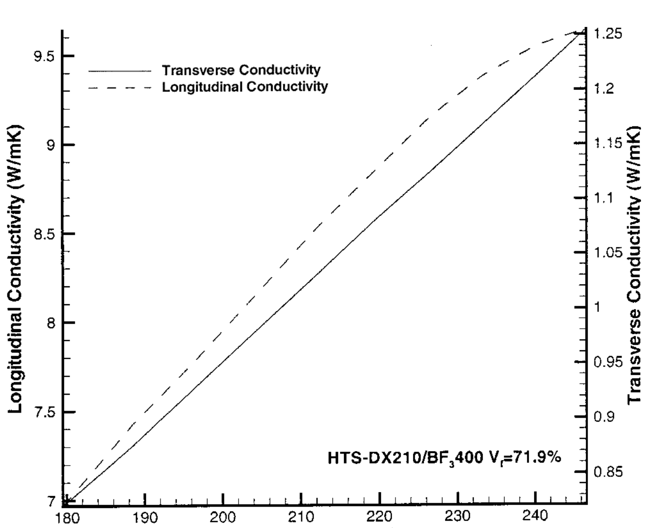

b) Conductivity variations along bar

Fig. 11 Multiscale bar results.

where

$$k(T) = 3.0194x10^{-3} + 0.15692T - 1.9159x10^{-3}T^2 + 1.0158x10^{-5}T^3 - 1.7535x10^{-8}T^4 \quad (17)$$

The conductivity data from which the curve fit was obtained are given by the rule of mixtures estimates at discrete temperatures. The comparisons here show that the AEH results for a simple unidirectional composite agree well with the one-dimensional analytical results.

The conductivity changes along the length of the one dimension, which is permissible in the AEH approach due to the associated localization that provides the coupling between the length scales. The temperature-dependent conductivities in Fig. 11b are comparable with the available experimental data in Fig. 9. Such a consolidated approach, wherein conductivity variations within a single problem occur, is not feasible with existing analytical formulas or numerical methods in as general a way as shown here.

The solution procedure begins with an initial assumed solution of the macrolevel temperature distribution. For each macroelement, the average centroid temperature and temperature gradients are computed, and then the localized temperatures in each microelement are obtained from the first two terms in Eq. (4) and from Eq. (11). From the microtemperatures, the constituent conductivities are obtained. The solution for χ in Eq. (12) is then obtained iteratively. Once a converged solution is obtained for the microequation, the effective conductivity for the macroelement is obtained from Eq. (15). These steps are then subsequently repeated for each macroelement until the macrotemperature solutions converge as well.

Conclusions

Recent developments in composite manufacturing simulations and in situ mechanics analyses have shown that multiple scales must be considered for realistic modeling. It is not sufficient to consider the scales independently. Efforts in the past were restricted to homogenization with the necessary localization performed in heuristic ways. In contrast to most of the homogenization techniques, AEH provides a mathematically rigorous procedure for performing localization that makes it suitable for nonlinear problems where the microstructural constituent properties are dependent on the macrolevel, global solution. Yet, despite the demonstrated utility of the AEH approach thus far, it has not been apparent from existing literature how the method is to be implemented for nonlinear situations and how it compares to other analytical and experimental results.

To further investigate and demonstrate the AEH method and to evaluate the most cost-effective method of obtaining nonlinear homogenized conductivities, two AEH approaches were explored. The first approach employed a simple linearized localization where the temperature over the microscale is uniform and equal to the average macroelement temperature. The microequations for this method are, therefore, linear. The second method assumed that the temperatures at the microscale are nonuniform. The findings indicate two conclusions. The first is that in most problems the sensitivity to the higher-order term is nominal. This is reflected in the very small difference in the computed conductivity for the asymmetric fiber example. The second conclusion, which is a consequence of the first, is that problems involving shallow temperature gradients and mildly asymmetric fibers can employ a linearized homogenization approach to capture nonlinear microeffects without significant loss of accuracy while decreasing computational effort.

The AEH approach was also compared favorably with available analytical and experimental literature. Using existing experiments that provide both effective and constituent conductivities at various temperatures, the temperature-dependent conductivity predictions were validated. Volume fraction variations were also considered. Better agreement is expected for problems in which the constituent material properties are obtained independently from the effective properties, but it is understood that this may be difficult from an experimental point of view. All of the measurement data used for comparison purposes in this paper used rule of mixtures equations to backcalculate the constituent properties from the experimentally determined effective properties.

Finally, an example multiscale problem was solved and the macrotemperature field was verified using a Runge–Kutta solution. The findings showed that for the simple problem, the AEH approach reverts to the conventional solution involving temperature-dependent conductivities. This verifies that the AEH approach converges to the degenerate problem for which existing data and solution techniques are available. For problems involving highly complex-shaped microstructures where material nonlinear issues are present, the AEH approach may be employed.

Acknowledgments

The authors are very pleased to acknowledge support in part by Battelle/U.S. Army Research Office, Research Triangle Park, North Carolina, under Grant DAAH04-96-C-0086 and by the Army High Performance Computing Research Center under the auspices of the Department of the Army, Army Research Laboratory (ARL) cooperative agreement number DAAH04-95-2-0003/Contract DAAH04-C-0008. Support in part by Andrew Mark of the Integrated Modeling and Testing Computational Technology Activity and the ARL/Major Shared Resource Center facilities is also gratefully acknowledged. Special thanks are also due to the Computational and Information Sciences Directorate at ARL, Aberdeen Proving Grounds, Maryland. Other related support in the form of computer grants from the Minnesota Supercomputer Institute, Minneapolis, Minnesota, and the Doctoral Dissertation Fellowship from the University of Minnesota is also gratefully acknowledged.

References

[1]Bensoussan, A., Lions, J. L., and Papanicolaou, G., *Asymptotic Analysis for Periodic Structures*, North-Holland, New York, 1978, Chap. 1.

[2]Sanchez-Palencia, E., *Non-Homogeneous Media and Vibration Theory*, Lecture Notes in Physics, Vol. 127, Springer-Verlag, Berlin, 1980, Chap. 5.

[3]Bendsöe, M. P., and Kikuchi, N., "Generating Optimal Topologies in Structural Design Using a Homogenization Method," *Computer Methods in Applied Mechanics and Engineering*, Vol. 71, No. 2, 1988, pp. 197–224.

[4]Lene, F., "Damage Constitutive Relations for Composite Materials," *Engineering Fracture Mechanics*, Vol. 25, No. 5/6, 1986, pp. 713–728.

[5]Fish, J., and Shek, K., "Computational Plasticity and Viscoplasticity for Composite Materials and Structures," *Composites Part B: Engineering*, Vol. 29, No. 5, 1998, pp. 613–619.

[6]Suquet, P., "Local and Global Aspects in the Mathematical Theory of Plasticity," *Plasticity Today—Modeling Methods and Applications*, edited by A. Sawczuk and G. Bianchi, Elsevier, New York, 1985, pp. 279–310.

[7]Terada, K., and Kikuchi, N., "Nonlinear Homogenization Method for Practical Applications," *Computational Methods in Micromechanics*, Applied Mechanics Div. 212, American Society of Mechanical Engineers, 1995, Fairfield, NJ, pp. 1–16.

[8]Chung, P. W., Namburu, R. R., and Tamma, K. K., "Three-Dimensional Elasto–Plastic Heterogeneous Media Subjected to Short Transient Loads," AIAA Paper 99-1239, April 1999.

[9]Dasgupta, A., and Agarwal, R. K., "Orthotropic Thermal Conductivity of Plain-Weave Fabric Composites Using a Homogenization Technique," *Journal of Composite Materials*, Vol. 26, No. 18, 1992, pp. 2736–2758.

[10]Chang, W., and Kikuchi, N., "Analysis of Non-Isothermal Mold Filling Process in Resin Transfer Molding (RTM) and Structural Reaction Injection Molding (SRIM)," *Computational Mechanics*, Vol. 16, No. 1, 1995, pp. 22–35.

[11]Pilling, M. W., Yates, B., Black, M. A., and Tattersall, P., "The Thermal Conductivity of Carbon Fibre-Reinforced Composites," *Journal of Materials Science*, Vol. 14, 1979, pp. 1326–1338.

[12]Farmer, J. D., and Covert, E. E., "Thermal Conductivity of a Thermosetting Advanced Composite During Its Cure," *Journal of Thermophysics and Heat Transfer*, Vol. 10, No. 3, 1996, pp. 467–475.

[13]Springer, G. S., and Tsai, S. W., "Thermal Conductivities of Unidirectional Materials," *Journal of Composite Materials*, Vol. 1, No. 1, 1967, pp. 166–173.

[14]Rolfes, R., and Hammerschmidt, U., "Transverse Thermal Conductivity of CFRP Laminates: A Numerical and Experimental Validation of Approximation Formulae," *Composite Science and Technology*, Vol. 54, No. 1, 1995, pp. 45–54.

[15]Lewis, T. B., and Nielsen, L. E., "Viscosity of Dispersed and Aggregated Suspensions of Spheres," *Transactions of the Society of Rheology*, Vol. 12, 1968, pp. 421–443.

[16]Polder, D., and van Santen, J. H., "The Effective Permeability of Mixtures of Solids," *Physika*, Vol. 12, 1946, pp. 257–269.

[17]Lord Rayleigh, "On the Influence of Obstacles Arranged in Rectangular Order Upon the Properties of a Medium," *Philosophical Magazine Series 5*, Vol. 34, 1882, pp. 481–502.